

## Supplementary information

### Unusual mode of protein binding by a cytotoxic $\pi$ -arene ruthenium(II) piano-stool compound containing an O,S-chelating ligand

5

Jana Hildebrandt,<sup>a</sup> Helmar Görls,<sup>a</sup> Norman Häfner,<sup>b</sup> Giarita Ferraro,<sup>c</sup> Matthias Dürst,<sup>b</sup> Ingo B. Runnebaum,<sup>b</sup> Wolfgang Weigand,<sup>a,\*</sup> and Antonello Merlino<sup>c,d,\*</sup>

#### Materials and Methods

#### 10 Synthesis and characterization of Compound 1

Crystal structure determination

Cytotoxicity

UV-Vis absorption spectroscopy

Crystallization, X-ray diffraction data collection, structure resolution and refinement of RNase A-Compound 1 adduct

#### 15 References

Table S1. Crystal data and structure refinement for Compound 1

Table S2. Bond lengths [Å] and angles [°] for Compound 1

Table S3. Selected distances and angles of Compound 1 compared to L

#### 20 Table S4. Data collection and refinement statistics of the RNase A-Compound 1 adduct

Figure S1. UV-Vis spectra of 0.3 mM Compound 1 under different experimental conditions followed each 1 h over 24 h. (A) 100 % DMSO; (B) 50 % DMSO; 50 % PBS pH 7.4. (C) 10 mM sodium citrate pH 5.1; (D) 10 mM sodium citrate pH 5.1, protein:metallodrug ratio 1:3; (E) 10 mM sodium citrate pH 5.1, protein:imidazole ratio 1:3;

#### 25 UV/Vis spectra of Compound 1 in DMSO show an intense peak at 346 nm, a small peak at 296 nm and a shoulder at 457 nm. The Compound experiences a slow red shift of its main band up to 354 nm, accompanied by a progressive slow decrease in intensity of all bands of the spectrum.

UV/Vis spectra of Compound 1 in PBS pH 7.4 show a similar behaviour when compared to the spectra of the compound in DMSO, although changes in the spectra are less pronounced. Peaks are observed at 295 nm and at 345 nm. Shoulder at 450 nm.

#### 30 UV/Vis spectra of Compound 1 in sodium citrate pH 5.1 show an intense peak at 342 nm, a small peak at 293 nm and a shoulder at 450 nm. Within 24 h, the complex experiences a red shift of its major band up to 346 nm and a blue shift of the band at 293 nm which disappears upon 24 h and of the shoulder to 431 nm. The observed spectral changes are different in the presence of the protein. In fact, Compound 1 spectra in the presence of RNase A show a major peak at 346 nm and a very small peak at 457 nm that decrease their intensity with time. The peak at 293 nm is overlapped with that of the protein at 280 nm. After 24 h a red shift of the band at 346 nm is observed also in this case.

#### 35 Figure S2. UV-Vis spectra of 1 mM Compound 1 in 90% PBS at pH 7.4, 10% DMSO, 1M NaCl, followed each 1 h over 24 h. These spectra should be compared to those reported in Figure 2B.

Figure S3. UV-Vis spectra of 1 mM Compound 1 followed each 1 h over 24 h in 90% PBS at pH 7.4, 10% DMSO in the presence of 5'-GMP

#### 40 Figure S4. Hydrolysis of yeast RNA (evaluated by measuring the variation of absorbance at 300 nm as function of time upon addition of the protein to the yeast RNA sample) by RNase A (black) and its adducts with Compound 1. Catalytic activity of RNase A in the presence of Compound 1 at different protein to metal ratio was determined spectrophotometrically by using the Kunitz assay [19]. 0.5 mg x mL<sup>-1</sup> of RNA and enzyme concentration = 0.5 µg x mL<sup>-1</sup> were used in 50 mM sodium citrate buffer pH 5.1, at 298 K. Spectrophotometric measurements were performed with a Jasco spectrophotometer. Experiments have been performed after 24 h of incubation. Protein remains well active in the presence of the compound.

#### 45 Figure S5. Compound 1 binding site in RNase A-Compound 1 adduct showing the Ru centre bound to His105. Anomalous electron density map that allows the identification of Ru centre is shown at 4σ level.

Figure S6. Details of Compound 1 binding site in molecule A of RNase A-Compound 1 adduct showing the Ru centre bound to His105. 2Fo-Fc electron density maps are contoured at 5σ (red) and 0.8σ (cyan) level.

50

## Materials and Methods

### Synthesis and characterization of Compound 1

The  $\beta$ -hydroxy dithiocinnamic methyl ester and  $[(\eta^6-p\text{-cymene})\text{RuCl}_2]_2$  were prepared using protocols available in literature, with minor modifications.  $[(\eta^6-p\text{-cymene})\text{RuCl}_2]_2$  (0.5 equiv, 500 mg, 0.81 mmol) was dissolved in 50 mL tetrahydrofuran (THF). The  $\beta$ -hydroxy dithiocinnamic methyl ester (1 equiv, 367 mg, 1.62 mmol) was dissolved in 25 mL THF. Potassium-*tert*-butoxylate (*t*-BuOK, 2 equiv, 182 mg, 1.62 mmol) was added to that solution and stirred 30 min at room temperature (r.t.). The solution of the deprotonated ligand was added dropwise to the suspension of  $[(\eta^6-p\text{-cymene})\text{RuCl}_2]_2$  and stirred at rt for 24 h. After adding sulfuric acid ( $\text{H}_2\text{SO}_4$ , 20 ml, 2M) to the solution, the mixture was stirred for 30 min and afterwards extracted with dichloromethane (DCM, 3 x 30 mL). The combined organic phases were washed with water (3 x 20 mL) and dried over sodium sulfate. After filtration and evaporation of the solvent, the crude product was purified with column chromatography. Column chromatography mobile phase: DCM - DCM 10:THF 1 - THF. Yield: 190 mg (23.6%) as red crystals.  $^1\text{H}$  NMR (600 MHz,  $\text{CD}_2\text{Cl}_2$ ):  $\delta$  = 1.26 (d,  $^3J_{\text{H-H}}=6.4$  Hz, 6H, -cymene-CH-( $\text{CH}_3$ )<sub>2</sub>); 2.20 (s, 3H,  $\text{CH}_3$ , -cymene- $\text{CH}_3$ ); 2.64 (s, 3H, -SCH<sub>3</sub>); 2.83 (sp, 1H, -cymene-CH-( $\text{CH}_3$ )<sub>2</sub>); 5.33 (m, 2H, -cymene:CH<sub>3</sub>-C-CH-CH-C-CH-( $\text{CH}_3$ )<sub>2</sub>); 5.52 (m, 2H -cymene:CH<sub>3</sub>-C-CH-CH-C-CH-( $\text{CH}_3$ )<sub>2</sub>); 6.71 (s, 1H, =CH); 6.85 (m, 2H, -Ar-*o*-H); 7.11 (m, 1H, -Ar-*m*-H); 7.23 (m, 3H, =CH/ -Ar-*p*-H); 10.1 (s, 1H, -COH).  $^{13}\text{C}\{^1\text{H}\}$  NMR (101 MHz,  $\text{CD}_2\text{Cl}_2$ ):  $\delta$  = 17.6 (-SCH<sub>3</sub>); 18.3 (-cymene-C-CH<sub>3</sub>); 22.4 (-cymene-CH-( $\text{CH}_3$ )<sub>2</sub>); 30.9 (-cymene-CH-( $\text{CH}_3$ )<sub>2</sub>); 83.3 (-cymene:CH<sub>3</sub>-C-CH-CH-C-CH-( $\text{CH}_3$ )<sub>2</sub>); 83.8 (CH<sub>3</sub>-C-CH-CH-C-CH-( $\text{CH}_3$ )<sub>2</sub>); 85.5 (CH<sub>3</sub>-C-CH-CH-C-CH-( $\text{CH}_3$ )<sub>2</sub>); 85.6 (CH<sub>3</sub>-C-CH-CH-C-CH-( $\text{CH}_3$ )<sub>2</sub>); 100.8 (CH<sub>3</sub>-C-CH-CH-C-CH-( $\text{CH}_3$ )<sub>2</sub>); 102.3 (CH<sub>3</sub>-C-CH-CH-C-CH-( $\text{CH}_3$ )<sub>2</sub>); 109.2 (=CH); 125.2 (-Ar-*m*-C); 129.2 (-Ar-*o*-C); 129.4 (-COH); 156.9 (-Ar-*p*-C); 178.0 (-ArC1); 187.3 (-C-O-); 207.2 (-C=S). MS (DEI): *m/z* = 134, 119, 115, 91, 77, 39, 28. Elemental analysis: calculated for  $\text{C}_{20}\text{H}_{23}\text{ClO}_2\text{RuS}_2$  C: 48.43%; H: 4.67%; S: 12.93%, found: C: 48.33%; H: 4.83%; S: 12.42%.

### Crystal structure determination

To obtain single crystals of Compound 1, the sample was dissolved in a DCM solution after addition of a few drop of methanol. Crystals were grown by slow evaporation of the solvent. X-ray diffraction data were collected at University of Jena using a Nonius KappaCCD diffractometer and graphite-monochromated Mo- $K_\alpha$  radiation. The intensity data were collected on a Nonius KappaCCD diffractometer, using graphite-monochromated Mo- $K_\alpha$  radiation. Data were corrected for Lorentz and polarization effects; absorption was taken into account on a semi-empirical basis using multiple-scans [1-3]. The structure was solved by direct methods (SHELXS [4]) and refined by full-matrix least squares techniques against  $F_o^2$  (SHELXL-97 [4]). All hydrogen atoms were located by difference Fourier synthesis and refined isotropically. All non-hydrogen atoms were refined anisotropically [4]. Crystallographic data and refinement statistics are reported in Table S1. Details on the structure are in Table S2. A comparison of selected bond lengths and angles of Compound 1 with data obtained for the ligand L are reported in Table S3. Crystallographic data for Compound 1 have been deposited at the Cambridge Crystallographic Data Centre under the accession code CCDC-1476883, They contain the supplementary crystallographic data excluding structure factors; these data can be obtained free of charge via [www.ccdc.cam.ac.uk/conts/retrieving.html](http://www.ccdc.cam.ac.uk/conts/retrieving.html) (or from the Cambridge Crystallographic Data Centre, 12, Union Road, Cambridge CB2 1EZ, UK; fax: (+44) 1223-336-033; or [deposit@ccdc.cam.ac.uk](mailto:deposit@ccdc.cam.ac.uk)).

### Cytotoxicity

The IC<sub>50</sub> values of Compound 1, L and Cisplatin was determined by means of the colorimetric MTT assay (MTT = 3-(4,5-dimethyl-2-thiazolyl)-2,5-diphenyl-2Htetrazolium bromide), CellTiter96 non-radioactive proliferation assay (Promega) [5]. For this purpose, cancer cell lines were cultured under standard conditions (5 % CO<sub>2</sub>, 37 °C, 90 % humidity) in RPMI medium supplemented with 10 % FCS, 100 U/ml penicillin and 100  $\mu\text{g}/\text{ml}$  streptomycin (Life Technologies, Germany). Cisplatin (Sigma, Germany) was freshly dissolved at 1 mg/ml in 0.9 % NaCl solution and diluted appropriately. Compound 1 and L were dissolved in dmsO. After seeding 5000 cells per well in a 96-well plate cells were allowed to attach for 24h and were incubated for 48h with different concentrations of the substances ranging from 0 to 500  $\mu\text{M}$  for Compound 1 and 0 to 1000  $\mu\text{M}$  for L tests. Each measurement was done in triplicate and repeated 3-times. The proportion of live cells was quantified by the MTT assay and after background subtraction relative values compared to the mean of medium controls were calculated. Non-linear regression analyses applying the Hill-slope were run in GraphPad 5.0 software. Platinum-resistant A2780 and SKOV3 cells were established by repeated rounds of three day incubations with increasing amounts of Cisplatin starting with 0.1  $\mu\text{M}$ . The concentration was doubled after three incubations interrupted by recovery phases with normal medium. Cells that survived the third round of 12.8  $\mu\text{M}$  Cisplatin were defined as resistant cultures. Analyzed control samples of non-tumorigenic cells included normal keratinocytes, normal fibroblasts and the immortal non-tumorigenic epithelial mammary gland cell line MCF-10A. Primary keratinocytes and fibroblasts were isolated from two individual human foreskins. Cultures of normal cells were used at early passages still showing cell proliferation.

### UV-Vis absorption spectroscopy

UV-vis spectra of Compound 1 were recorded at room temperature on a Varian Cary 5000 UV-Vis-NIR spectrophotometer using 1 cm path length cuvette. The spectra were collected in the 240-700 nm range every 1 nm at a scan rate of 600 nm min<sup>-1</sup>. The

spectral profile of Compound **1** was analysed under different experimental conditions: in pure DMSO, in a 50% DMSO and 50% PBS pH 7.4 solution and in 10 mM sodium citrate, in the absence and in the presence of RNase A (protein to metal ratio 1:3), that was the condition used to grow protein crystals.

## 5 Crystallization, X-ray diffraction data collection, structure resolution and refinement of RNase A-Compound **1** adduct

Crystals of RNase A were obtained as previously described [6]. Crystals of the adduct were obtained by soaking procedure (4 days) as described in previous works [7-8]. Briefly, 1  $\mu$ L solution of Compound **1** dissolved in DMSO was mixed with an equal amount of precipitant solution. Then, half of the resulting solution was added to the drop containing crystals of RNase A. After four days of soaking, X-ray diffraction data were collected at the CNR Institute of Biostructures and Bioimages, using a Saturn944 CCD detector  
10 equipped with CuK $\alpha$  X-ray radiation from a Rigaku Micromax 007 HF generator. Crystals were dehydrated [10] and data collection was performed without addition of cryoprotectants [9]. Data sets were processed, merged and scaled using Mosflm [11]. Data collection statistics are reported in Table S1.

The structure was solved by molecular replacement method, using protein atoms of chain A from pdb file 1JVT [12] as a starting model and the program Phaser [13]. Structure was refined with Refmac5.7 [14]. Model building, addition of ligands and inspection of electron  
15 density maps were performed using Coot [15]. The electron density map is very well defined for all residues of the two molecules in the asymmetric unit with exceptions of the regions encompassing residues 16-22 that are rather disordered in both the two chains. Model refines against data to 1.79  $\text{\AA}$  resolution with Rfactor and Rfree values of 17.9 and 23.6 %. The model was also refined against all the data collected with CC $_{1/2}$ >0.3 following the indications of Diederichs and Karplus [16-17], up to 1.51  $\text{\AA}$  resolution, with Rfactor and Rfree values of 17.8 and 23.9 %. However at this resolution the completeness is too low (overall completeness=60.6%), and thus the  
20 model refined and the structure factors at 1.79  $\text{\AA}$  resolution were deposited in the Protein Data Bank (PDB code 5JLG). Refinement statistics are reported in Table S1. Structure validations were carried out using Whatcheck [18]. Final structure has 3 residues in the disallowed region of the Ramachandran plot, which correspond to Ser22 and Gln60 in the chain A, Ser16 in the chain B. In the Fo-Fc electron density maps there are just five peaks > 5  $\sigma$  uninterpreted. Four out of these peaks could correspond to solvent molecules alternative to Compound **1** fragment bound to the protein.

25

### References

1. COLLECT, Data Collection Software; Nonius B.V., Netherlands, 1998
2. Z. Otwinowski & W. Minor, „Processing of X-Ray Diffraction Data Collected in Oscillation Mode“, in Methods in Enzymology, Vol. 276, Macromolecular Crystallography, Part A, edited by C.W. Carter & R.M. Sweet, pp. 307-326,  
30 Academic Press, San Diego, USA, 1997
3. SADABS 2.10, Bruker-AXS inc., 2002, Madison, WI, U.S.A
4. Sheldrick, G. M. *Acta Cryst.* (2008). A46, 112-122.
5. T. Mosmann. *Journal of Immunological Methods* **65** (1-2): 55-63.
6. L. Vitagliano, A. Merlino, A. Zagari, L. Mazzarella. *Proteins Sci* 2000, **9**, 1217-1225.
- 35 7. L. Messori, A. Merlino. *Inorg. Chem.* 2014, **53**, 3929-3931.
8. L. Messori, T. Marzo, E. Michelucci, I. Russo Krauss, C. Navarro-Ranninger, A. G. Quiroga, A. Merlino. *Inorg Chem.* 2014, **53**, 7806-7808.
9. I. Russo Krauss, F. Sica, C.A. Mattia, A. Merlino. *Int J Mol Sci.* 2012, **13**, 3782-3800.
10. E. Pellegrini, D. Piano, M. W. Bowler. *Acta Crystallogr D Biol Crystallogr.* 2011, **67**, 902-906.
- 40 11. T. G. G. Battye, L. Kontogiannis, O. Johnson, H. R. Powell, A. G. W. Leslie. *Acta Crystallogr D Biol Crystallogr.* 2011, **67** (Pt 4), 271-281.
12. L. Vitagliano, A. Merlino, A. Zagari, L. Mazzarella. *Proteins* 2002, **46**, 97-104
13. A. J. McCoy, R.W.Grosse-Kunstleve, P. D. Adams, M. D. Winn, L.C. Storoni, R.J. Read. *J Appl Crystallogr.* 2007, **40**, 658-674.
14. G. N. Murshudov, P. Skubak, A. A. Lebedev, N. S. Pannu, R. A. Steiner, R. A. Nicholls, M. D. Winn, F. Long, A. A. Vagin, *Acta*  
45 *Crystallogr., Sect. D: Biol. Crystallogr.* 2011, **67**, 355-367.
15. P. Emsley, B. Lohkamp, W. G. Scott, K. Cowtan. *Acta Crystallogr D Biol Crystallogr.* 2010, **66**, 486-501.
16. P.A. Karplus, K. Diederichs. *Science* 2012, **336**(6084), 1030-1033.
17. K. Diederichs, P.A. Karplus *Acta Crystallogr D Biol Crystallogr.* 2013, **69** (Pt 7), 1215-1222.
18. R.W.W. Hoof, G. Vriend, C. Sander, E. E. Abola, *Nature* 1996, **381**, 272.
- 50 19. M. Kunitz. *J. Biol. Chem.* 1946, **164**, 563-568.

**Table S1.** Crystal data and structure refinement for Compound 1.

Compound 1	
Empirical formula	C <sub>20</sub> H <sub>23</sub> Cl O <sub>2</sub> Ru S <sub>2</sub>
Formula weight	496.02
5 Temperature	133(2) K
Wavelength	0.71073 Å
Crystal system	Orthorhombic
Space group	Pna2(1)
Unit cell dimensions	a = 22.1070(4) Å
10	b = 11.4122(2) Å
	c = 7.9006(1) Å
Volume	1993.24(6) Å <sup>3</sup>
Z	4
Density (calculated)	1.653 Mg x m <sup>-3</sup>
15 Absorption coefficient	1.142 mm <sup>-1</sup>
F(000)	1008
Crystal size	0.042 x 0.038 x 0.012 mm <sup>3</sup>
θ range for data collection	3.27 to 27.49°.
Index ranges	-28<=h<=28, -14<=k<=14, -10<=l<=8
20 Reflections collected	13265
Independent reflections	4028 [R(int) = 0.0207]
Completeness to θ = 27.49°	99.6 %
Absorption correction	Semi-empirical from equivalents
Max. and min. transmission	0.7456 and 0.6881
25 Refinement method	Full-matrix least-squares on F <sup>2</sup>
Data / restraints / parameters	4028 / 1 / 327
Goodness-of-fit on F <sup>2</sup>	1.070
Final R indices [I>2σ(I)]	R1 = 0.0149, wR2 = 0.0362
R indices (all data)	R1 = 0.0151, wR2 = 0.0364
30 Absolute structure parameter	-0.012(18)
Largest diff. peak and hole	0.236 and -0.284 e <sup>-</sup> x Å <sup>-3</sup>

**Table S2.** Bond lengths [ $\text{\AA}$ ] and angles [ $^\circ$ ] for Compound **1**.

---

	Ru(1)-O(1)	2.0538(12)
	Ru(1)-C(15)	2.1644(18)
5	Ru(1)-C(16)	2.1717(19)
	Ru(1)-C(12)	2.175(2)
	Ru(1)-C(11)	2.1984(19)
	Ru(1)-C(13)	2.208(2)
	Ru(1)-C(14)	2.2351(19)
10	Ru(1)-S(1)	2.3415(4)
	Ru(1)-Cl(1)	2.4374(6)
	S(1)-C(1)	1.6892(19)
	S(2)-C(1)	1.7614(19)
	S(2)-C(10)	1.800(2)
15	O(1)-C(3)	1.268(2)
	O(2)-C(6)	1.364(3)
	O(2)-H(1O2)	0.78(3)
	C(1)-C(2)	1.381(2)
	C(2)-C(3)	1.407(3)
20	C(2)-H(2)	0.93(2)
	C(3)-C(4)	1.502(2)
	C(4)-C(9)	1.389(3)
	C(4)-C(5)	1.396(3)
	C(5)-C(6)	1.393(2)
25	C(5)-H(5)	0.94(2)
	C(6)-C(7)	1.391(3)
	C(7)-C(8)	1.379(3)
	C(7)-H(7)	0.94(2)
	C(8)-C(9)	1.397(3)
30	C(8)-H(8)	0.86(3)
	C(9)-H(9)	0.99(3)
	C(10)-H(10C)	0.94(3)
	C(10)-H(10B)	0.95(3)
	C(10)-H(10A)	0.94(3)
35	C(11)-C(12)	1.413(3)
	C(11)-C(16)	1.427(3)
	C(11)-C(18)	1.513(3)
	C(12)-C(13)	1.425(3)
	C(12)-H(12)	0.94(2)
40	C(13)-C(14)	1.397(3)
	C(13)-H(13)	0.97(2)
	C(14)-C(15)	1.425(3)
	C(14)-C(17)	1.507(3)
	C(15)-C(16)	1.402(3)
45	C(15)-H(15)	0.96(3)
	C(16)-H(16)	0.90(2)
	C(17)-H(17C)	0.94(3)
	C(17)-H(17B)	1.02(3)
	C(17)-H(17A)	0.92(4)
50	C(18)-C(19)	1.522(3)
	C(18)-C(20)	1.529(3)
	C(18)-H(18)	0.96(2)
	C(19)-H(19B)	0.91(3)
	C(19)-H(19A)	1.00(4)
55	C(19)-H(19C)	0.91(3)
	C(20)-H(20C)	0.92(3)
	C(20)-H(20B)	0.94(3)
	C(20)-H(20A)	0.96(3)

	O(1)-Ru(1)-C(15)	148.69(7)
	O(1)-Ru(1)-C(16)	159.40(7)
	C(15)-Ru(1)-C(16)	37.74(8)
5	O(1)-Ru(1)-C(12)	92.70(7)
	C(15)-Ru(1)-C(12)	80.20(8)
	C(16)-Ru(1)-C(12)	67.69(8)
	O(1)-Ru(1)-C(11)	121.59(6)
	C(15)-Ru(1)-C(11)	68.81(7)
10	C(16)-Ru(1)-C(11)	38.11(7)
	C(12)-Ru(1)-C(11)	37.70(7)
	O(1)-Ru(1)-C(13)	88.70(6)
	C(15)-Ru(1)-C(13)	66.97(8)
	C(16)-Ru(1)-C(13)	79.60(7)
15	C(12)-Ru(1)-C(13)	37.92(8)
	C(11)-Ru(1)-C(13)	68.36(7)
	O(1)-Ru(1)-C(14)	111.41(7)
	C(15)-Ru(1)-C(14)	37.76(8)
	C(16)-Ru(1)-C(14)	68.07(8)
20	C(12)-Ru(1)-C(14)	67.76(9)
	C(11)-Ru(1)-C(14)	81.28(7)
	C(13)-Ru(1)-C(14)	36.63(8)
	O(1)-Ru(1)-S(1)	90.25(4)
	C(15)-Ru(1)-S(1)	120.41(6)
25	C(16)-Ru(1)-S(1)	92.71(6)
	C(12)-Ru(1)-S(1)	115.64(6)
	C(11)-Ru(1)-S(1)	89.84(5)
	C(13)-Ru(1)-S(1)	153.39(6)
	C(14)-Ru(1)-S(1)	158.17(6)
30	O(1)-Ru(1)-Cl(1)	83.54(4)
	C(15)-Ru(1)-Cl(1)	90.63(6)
	C(16)-Ru(1)-Cl(1)	116.90(6)
	C(12)-Ru(1)-Cl(1)	155.81(6)
	C(11)-Ru(1)-Cl(1)	154.81(5)
35	C(13)-Ru(1)-Cl(1)	117.93(6)
	C(14)-Ru(1)-Cl(1)	91.32(6)
	S(1)-Ru(1)-Cl(1)	88.333(19)
	C(1)-S(1)-Ru(1)	110.14(7)
	C(1)-S(2)-C(10)	104.65(9)
40	C(3)-O(1)-Ru(1)	134.09(11)
	C(6)-O(2)-H(1O2)	113(2)
	C(2)-C(1)-S(1)	129.20(15)
	C(2)-C(1)-S(2)	113.15(14)
	S(1)-C(1)-S(2)	117.59(10)
45	C(1)-C(2)-C(3)	127.12(17)
	C(1)-C(2)-H(2)	115.9(15)
	C(3)-C(2)-H(2)	116.8(15)
	O(1)-C(3)-C(2)	126.18(15)
	O(1)-C(3)-C(4)	113.91(15)
50	C(2)-C(3)-C(4)	119.90(16)
	C(9)-C(4)-C(5)	119.84(17)
	C(9)-C(4)-C(3)	123.85(18)
	C(5)-C(4)-C(3)	116.28(16)
	C(6)-C(5)-C(4)	120.29(18)
55	C(6)-C(5)-H(5)	117.8(13)
	C(4)-C(5)-H(5)	122.0(13)
	O(2)-C(6)-C(7)	118.38(17)
	O(2)-C(6)-C(5)	121.77(19)

	C(7)-C(6)-C(5)	119.84(19)
	C(8)-C(7)-C(6)	119.62(18)
	C(8)-C(7)-H(7)	120.9(13)
	C(6)-C(7)-H(7)	119.5(13)
5	C(7)-C(8)-C(9)	121.2(2)
	C(7)-C(8)-H(8)	120.1(18)
	C(9)-C(8)-H(8)	118.7(18)
	C(4)-C(9)-C(8)	119.2(2)
	C(4)-C(9)-H(9)	124.9(15)
10	C(8)-C(9)-H(9)	115.5(15)
	S(2)-C(10)-H(10C)	114.0(14)
	S(2)-C(10)-H(10B)	106.0(18)
	H(10C)-C(10)-H(10B)	107(2)
	S(2)-C(10)-H(10A)	114.9(17)
15	H(10C)-C(10)-H(10A)	101(2)
	H(10B)-C(10)-H(10A)	114(2)
	C(12)-C(11)-C(16)	116.93(18)
	C(12)-C(11)-C(18)	123.40(19)
	C(16)-C(11)-C(18)	119.61(17)
20	C(12)-C(11)-Ru(1)	70.23(12)
	C(16)-C(11)-Ru(1)	69.93(11)
	C(18)-C(11)-Ru(1)	128.16(13)
	C(11)-C(12)-C(13)	121.5(2)
	C(11)-C(12)-Ru(1)	72.07(12)
25	C(13)-C(12)-Ru(1)	72.33(13)
	C(11)-C(12)-H(12)	118.7(14)
	C(13)-C(12)-H(12)	119.7(14)
	Ru(1)-C(12)-H(12)	125.0(15)
	C(14)-C(13)-C(12)	121.26(19)
30	C(14)-C(13)-Ru(1)	72.72(12)
	C(12)-C(13)-Ru(1)	69.75(12)
	C(14)-C(13)-H(13)	121.0(14)
	C(12)-C(13)-H(13)	117.6(14)
	Ru(1)-C(13)-H(13)	126.6(14)
35	C(13)-C(14)-C(15)	117.52(18)
	C(13)-C(14)-C(17)	120.7(2)
	C(15)-C(14)-C(17)	121.6(2)
	C(13)-C(14)-Ru(1)	70.65(11)
	C(15)-C(14)-Ru(1)	68.43(11)
40	C(17)-C(14)-Ru(1)	128.30(16)
	C(16)-C(15)-C(14)	121.49(19)
	C(16)-C(15)-Ru(1)	71.41(11)
	C(14)-C(15)-Ru(1)	73.81(11)
	C(16)-C(15)-H(15)	120.3(14)
45	C(14)-C(15)-H(15)	117.6(14)
	Ru(1)-C(15)-H(15)	119.9(14)
	C(15)-C(16)-C(11)	121.24(18)
	C(15)-C(16)-Ru(1)	70.85(11)
	C(11)-C(16)-Ru(1)	71.96(10)
50	C(15)-C(16)-H(16)	120.0(16)
	C(11)-C(16)-H(16)	118.5(15)
	Ru(1)-C(16)-H(16)	126.0(16)
	C(14)-C(17)-H(17C)	108(2)
	C(14)-C(17)-H(17B)	112(2)
55	H(17C)-C(17)-H(17B)	116(3)
	C(14)-C(17)-H(17A)	113(2)
	H(17C)-C(17)-H(17A)	104(3)
	H(17B)-C(17)-H(17A)	103(4)

	C(11)-C(18)-C(19)	112.84(17)
	C(11)-C(18)-C(20)	109.64(17)
	C(19)-C(18)-C(20)	111.1(2)
	C(11)-C(18)-H(18)	107.6(14)
5	C(19)-C(18)-H(18)	109.4(14)
	C(20)-C(18)-H(18)	105.9(15)
	C(18)-C(19)-H(19B)	109.6(17)
	C(18)-C(19)-H(19A)	109.2(14)
	H(19B)-C(19)-H(19A)	108(3)
10	C(18)-C(19)-H(19C)	109.6(18)
	H(19B)-C(19)-H(19C)	109(2)
	H(19A)-C(19)-H(19C)	112(3)
	C(18)-C(20)-H(20C)	109(2)
	C(18)-C(20)-H(20B)	108.4(14)
15	H(20C)-C(20)-H(20B)	112(3)
	C(18)-C(20)-H(20A)	110.1(15)
	H(20C)-C(20)-H(20A)	107(2)
	H(20B)-C(20)-H(20A)	111(2)

---

20

**Table S3.** Selected distances [ $\text{\AA}$ ] and angles [ $^\circ$ ] of Compound **1** compared to those observed for **L**

	<b>L</b>	Compound <b>1</b>
O(1)-Ru(1)		2.0538(12)
S(1)-Ru(1)		2.3415(4)
Cl(1)-Ru(1)		2.4374(6)
O(1)-C(3)	1.330(6)	1.268(2)
C(3)-C(4)	1.477(6)	1.502(2)
S(1)-C(1)	1.662(5)	1.6892(19)
O(2)-C(8/6)	1.376(6)	1.364(3)
S(1)-Ru(1)-O(1)		90.25(4)
S(1)-Ru(1)-Cl(1)		88.333(19)
O(1)-Ru(1)-Cl(1)		83.54(4)

25

**Table S4.** Data collection and refinement statistics of the RNase A-Compound 1 adduct

		RNase A-Compound 1
	PDB code	5JLG
	Data collection temperature (K)	100
5	Data reduction	
	Space group	C2
	Unit cell parameters	
	a (Å)	100.47
	b (Å)	32.74
10	c (Å)	72.45
	$\beta$	90.06
	Molecules per asymmetric unit	2
	Observed reflections	57189
	Unique reflections	22643
15	Resolution (Å)	72.47-1.79 (1.83-1.79)
	Completeness (%)	78.7 (70.2)
	Rmerge (all I+ and I-)	0.064 (0.242)
	Rmerge in top intensity bin	0.047
	Rpim	0.050 (0.238)
20	I/ $\sigma$ (I)	10.5 (2.4)
	Multiplicity	2.9 (2.0)
	<i>Refinement</i>	
	Resolution (Å)	72.47-1.79
	number of reflections in working set	16805
25	number of reflections in test set	906
	R-factor/Rfree/Rall (%)	17.2/23.6/17.5
	Number of residues	2 x 124
	Non-H atoms used in the refinement	2373
	Mean B-value (Å <sup>2</sup> )	23.6
30	Ru atom occupancy	0.4, 0.5
	Ru atom B-factor (Å <sup>2</sup> )	27.7, 15.6
	Estimated overall coordinate errors	
	Rmsd bonds (Å)	0.015
	Rmsd angles (°)	1.74
35	Ramachandran values (%) from Coot	
	Preferred region	95.6
	Allowed	2.9 (number of residues:6)
	Disallowed	1.9 (number of residues:3)

Parentheses indicate information for highest resolution shell.

40

45

50

55

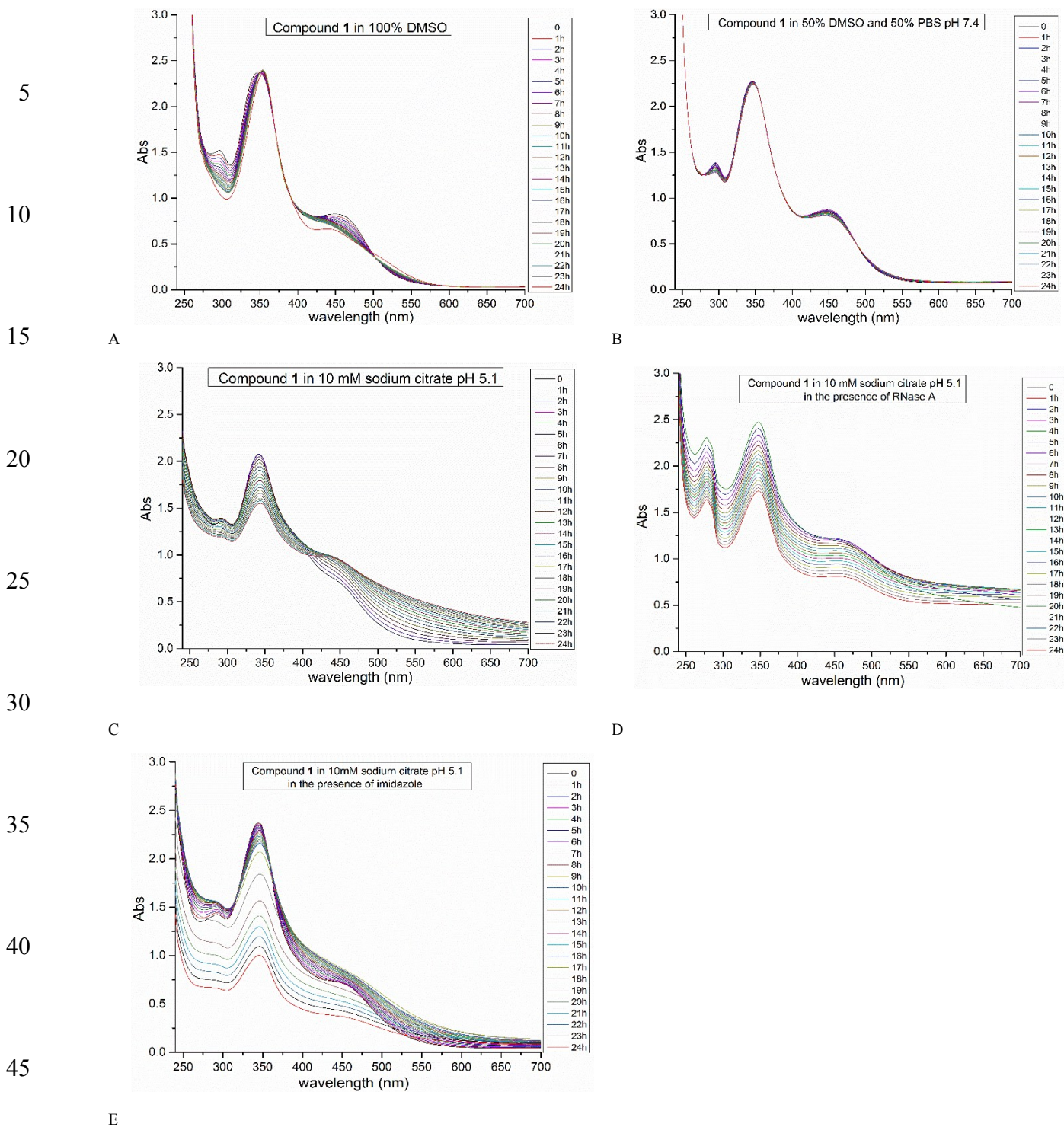


**Figure S1.** UV-Vis spectra of 0.3 mM Compound 1 under different experimental conditions followed each 1 h over 24 h. (A) 100 % DMSO; (B) 50 % DMSO; 50 % PBS pH 7.4. (C) 10 mM sodium citrate pH 5.1; (D) 10 mM sodium citrate pH 5.1, protein:metallodrug ratio 1:3; (E) 10 mM sodium citrate pH 5.1, protein:imidazole ratio 1:3;

UV/Vis spectra of Compound 1 in DMSO show an intense peak at 346 nm, a small peak at 296 nm and a shoulder at 457 nm. The Compound experiences a slow red shift of its main band up to 354 nm, accompanied by a progressive slow decrease in intensity of all bands of the spectrum.

UV/Vis spectra of Compound 1 in PBS pH 7.4 show a similar behaviour when compared to the spectra of the compound in DMSO, although changes in the spectra are less pronounced. Peaks are observed at 295 nm and at 345 nm. Shoulder at 450 nm.

5 UV/Vis spectra of Compound 1 in sodium citrate pH 5.1 show an intense peak at 342 nm, a small peak at 293 nm and a shoulder at 450 nm. Within 24 h, the complex experiences a red shift of its major band up to 346 nm and a blue shift of the band at 293 nm which disappears upon 24 h and of the shoulder to 431 nm. The observed spectral changes are different in the presence of the protein. In fact, Compound 1 spectra in the presence of RNase A show a major peak at 346 nm and a very small peak at 457 nm that decrease their intensity with time. The peak at 293 nm is overlapped with that of the protein at 280 nm. After 24 h a red shift of the band at 346 nm is observed also in this case.

5  
10  
15  
20  
25  
30  
35  
40  
45  
50

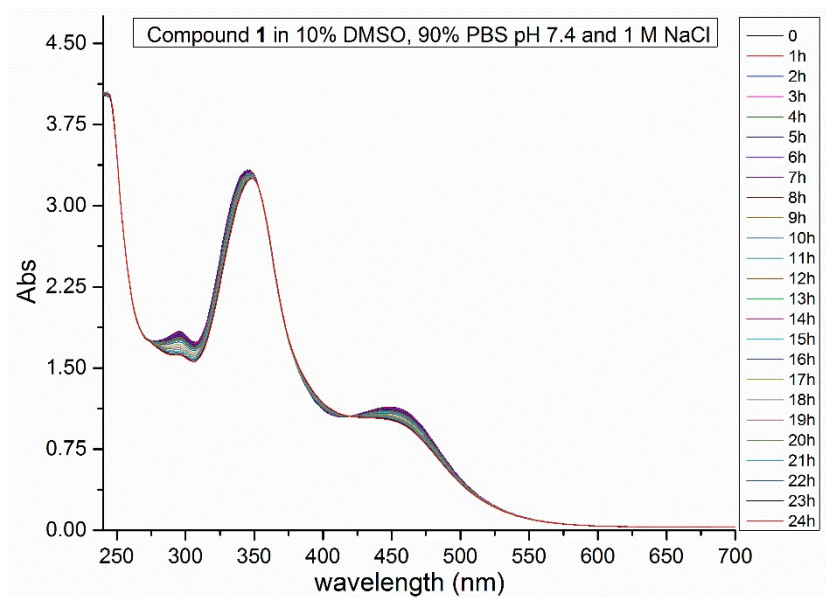


**Figure S2.** UV-Vis spectra of 1 mM Compound **1** in 90% PBS at pH 7.4, 10% DMSO, 1M NaCl, followed each 1 h over 24 h. These spectra should be compared to those reported in Figure 2B.

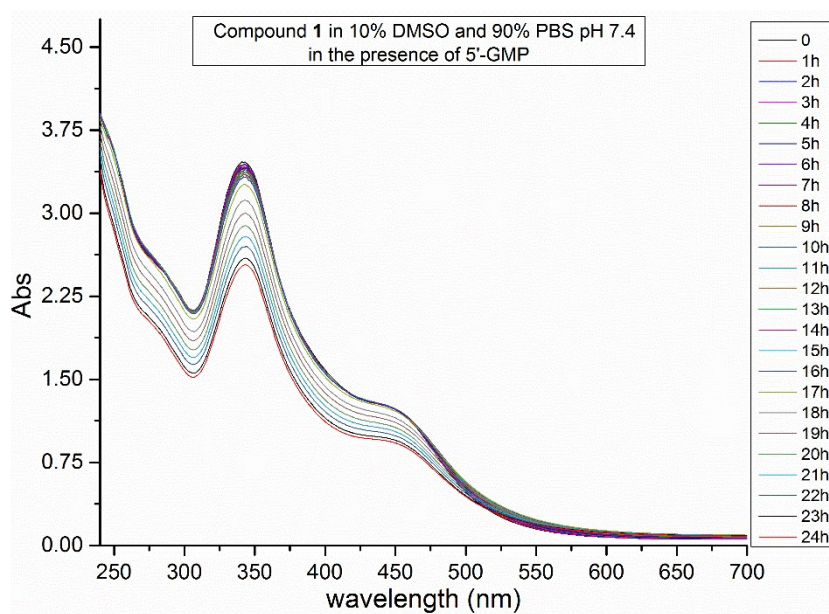
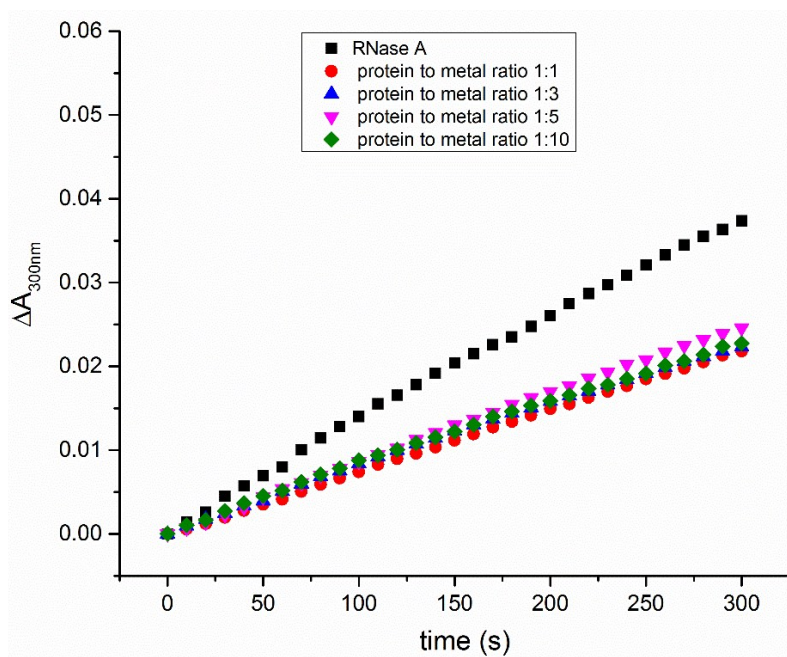


**Figure S3.** UV-Vis spectra of 1 mM Compound 1 followed each 1 h over 24 h in 10% DMSO and 90% PBS at pH 7.4, in the presence of 5'-GMP.

5

10

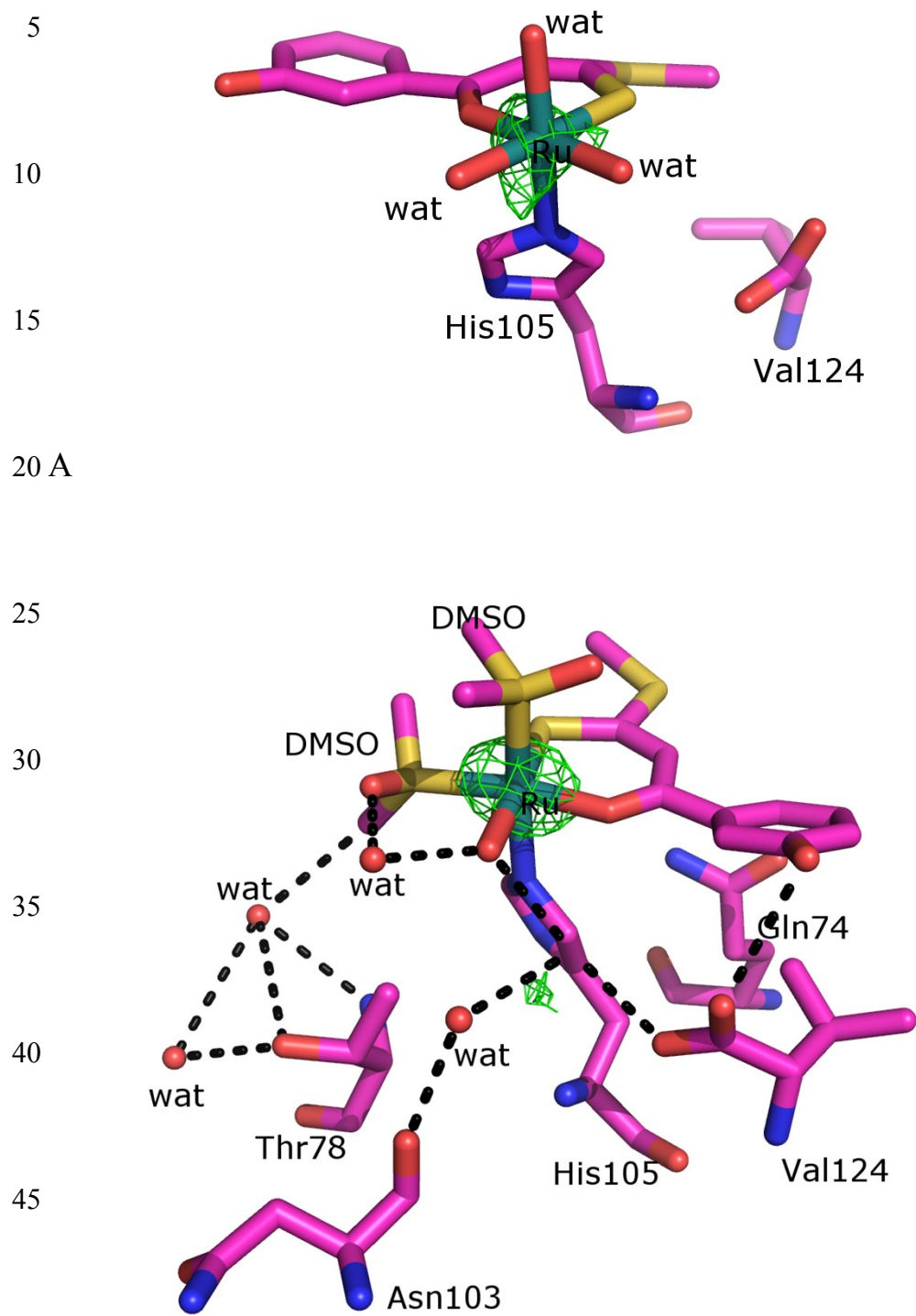
15



5 **Figure S4.** Hydrolysis of yeast RNA (evaluated by measuring the variation of absorbance at 300 nm as function of time upon addition of the protein to the yeast RNA sample) by RNase A (black) and its adducts with Compound **1**. Catalytic activity of RNase A in the presence of Compound **1** at different protein to metal ratio was determined spectrophotometrically by using the Kunitz assay [19]. 0.5 mg x mL<sup>-1</sup> of RNA and enzyme concentration =0.1 mg x mL<sup>-1</sup> were used in 50 mM sodium citrate buffer pH 5.1, at 298 K. Spectrophotometric measurements were performed with a Jasco spectrophotometer. Experiments have been performed after 24 h of

10 .

15



**B**

**Figure S5.** Compound 1 binding site in RNase A-Compound 1 adduct showing the Ru centre bound to His105. Anomalous electron density map that allows the identification of Ru centre is shown at  $4\sigma$  level.

5

10

15

20

25

30

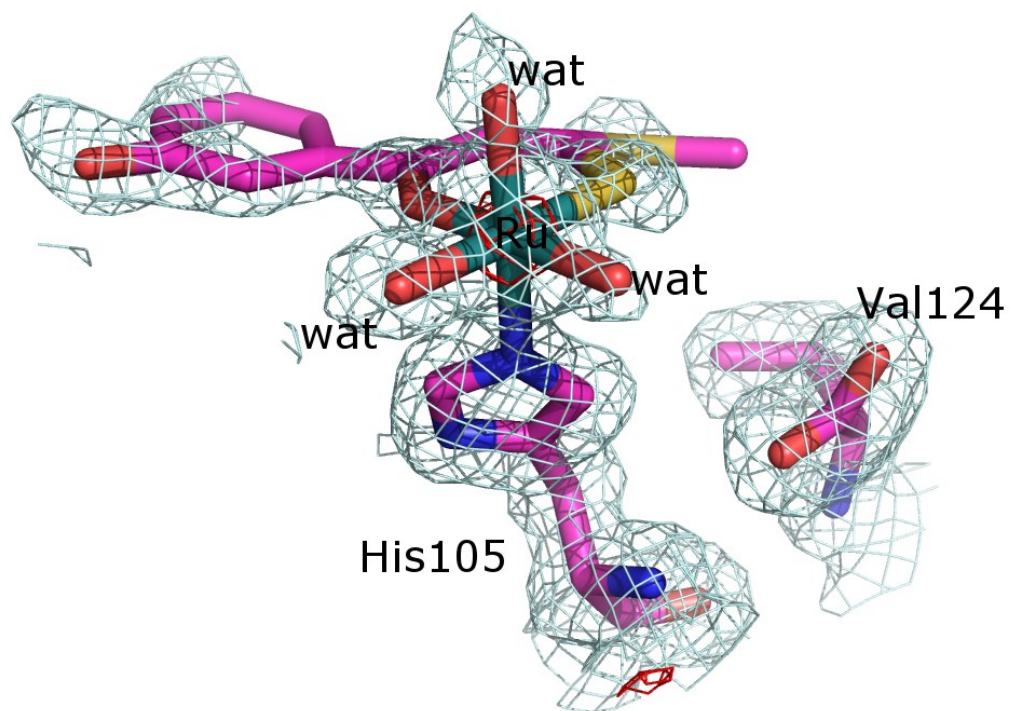


**Figure S6.** Details of Compound 1 binding site in molecule A of RNase A-Compound 1 adduct showing the Ru centre bound to His105. 35 2Fo-Fc electron density maps are contoured at 5 $\sigma$  (red) and 0.8 $\sigma$  (cyan) level.